

# Experimental Analysis of Single Slope Solar Still with Solar Dish Concentrator Using energy and Exergy Approach

**Maruthupandian, Yuvaraj; Esakkimuthu, Ganapathy Sundaram<sup>\*+</sup>**

*Department of Automobile Engineering, Velammal Engineering College, Chennai- INDIA*

**Vaithilingam, Sivakumar**

*Department of Mechanical Engineering, Ramco Institute of Technology, Rajapalayam, INDIA*

**Dhamodaran, Gopinath**

*Department of Mechanical Engineering, Velammal Engineering College, Chennai- INDIA*

**ABSTRACT:** The need for drinking water is increasing daily, and many research works have been carried out on converting seawater into drinking water. Natural conversion solar desalination systems were popular for producing fresh water, but the main constraint is their low yield. This paper discussed the performance variation of single slope solar still with four new different combinations proposed in this study with an objective to improve the solar still yield, i) With Insulation-Without Dish (WI-WoD), ii) Without Insulation-Without Dish (WoI-WoD), iii) Without Insulation-With Dish (WoI-WD) & iv) With Insulation-With Dish (WI-WD). The still was made up of stainless steel with an area of 0.25m<sup>2</sup>. The insulation was carried out with two layers of materials: the inner layer with thermocol and the outer layer with plywood. The bottom of the still was not insulated, and the solar concentrator dish was used to focus solar radiation on increasing the still water temperature, which led to an improved yield of the system. These experiments were conducted under the climatic condition of 13° 8' 58.05" N, 80° 11' 32.38" E, at Chennai, Tamilnadu, India. This study found that WI-WD produced the highest yield compared to other combinations. The WI-WD combination produced a 25.49% higher yield as compared to the conventional still (WI-WoD). The energy and exergy efficiency analysis were carried out for the WI-WD combination, and the values obtained are 30.06 and 1.6%, respectively. The WI-WD combination produced higher energy and exergy efficiencies compared to conventional still. The results state that the maximum hourly exergy destruction in basin liner, saline water, glass cover and dish concentrator are observed as 716.53, 53.82, 82.99 and 3836 W/m<sup>2</sup>, respectively.

**KEYWORDS:** Solar dish concentrator; Single slop solar still; Exergy & Energy analysis; exergy destruction.

## INTRODUCTION

One of the primary sources of energy for all life on earth is water. Water is the abundant liquid present

on the earth's surface. At the same time, humans cannot use the water from the sea directly due to the presence of

---

<sup>\*</sup>To whom correspondence should be addressed.

<sup>+</sup> E-mail: ganapathy\_sundar@yahoo.com

1021-9986/2023/10/3495-3510

16/\$/6.06

salinity. For the betterment of seawater usage for humans, the salt content must be removed from the seawater. One renewable method to separate the pure water from seawater is with a single slope natural conventional solar desalination system [1]. The solar desalination process has comparatively low efficiency with active methods. Many design and operational factors were proposed and implemented for the solar still desalination system to perform better like latitude, facing, slope angle, water depth, the thermal conductivity of the cover material, basin material, Insulation type, inlet water temperature, basin linear, gravels, stages of desalination, wind speed etc., Many researchers' works on Nanoparticles, Phase Change materials, fins, etc., to improve the yield of the solar still [2] [3].

*Kabeel et al.* studied the effect of latent heat storage and parabolic concentrator on passive solar desalination. They found that the yield increased 55-65% in the summer and 35-45% in the winter compared with usual solar still under Egyptian conditions [4]. *Osman et al.* compared a Fresnel Concentrating Solar Power (CSP) collector in a desalination plant with a plant entirely run by fossil fuel in Saudi Arabia's climatic conditions. They concluded that fuel breakeven cost falls from \$92/bbl to \$52/bbl after the use of the Fresnel concentrator; also, they recommended that the Fresnel concentrator with MED (Multi Effect Desalination) was more effective when operated without thermal energy storage material under specific climatic conditions [5]. *Alireza et al.* investigated the effect of a focal point concentrator in a solar desalination system with oil-based Nanofluids used as a solar working fluid. Different nanofluids were used as the working fluids, such as  $\text{Al}_2\text{O}_3/\text{oil}$ ,  $\text{Cu}/\text{oil}$ ,  $\text{CuO}/\text{oil}$ ,  $\text{TiO}_2/\text{oil}$ , and  $\text{MWCNT}/\text{oil}$ , to find the comparison performance in terms of yield. The  $\text{Cu}/\text{Oil}$  produced the maximum yield of 17.3 kg, and they concluded that the concentration level of nanoparticles improved the yield [6]. *Omara et al.* proposed an experimental setup with a solar dish concentrator with two axis tracking system coupled with a boiler in single-slope solar desalination. This proposed model still produces a maximum yield of 6.7  $\text{L}/\text{m}^2/\text{day}$  compared with the yield of conventional solar still of 1.5  $\text{L}/0.5\text{m}^2/\text{Day}$ . Without a pre-heater, the yield increased by 244%, while a pre-heater was used, the yield increased by 347% [7]. *Abubakkar et al.* investigated the dish solar concentrated hybrid with conventional solar still made up

of glass. The results discussed the variation of heat transfer in the side of stills and condenser glass with time [8]. *Saffa and Abdulkarim* proposed a new v-trough solar concentrator compared with the common parabolic trough collector in the solar desalination system. The experiment was carried out both indoors and outdoors using a solar simulator. This proposed v-trough achieves a thermal efficiency of up to 38% at the operating temperature of 100 °C. Small to medium-sized solar-powered water desalination systems can benefit greatly from this innovative design [9]. *Srithar et al.* investigated the triple basin solar still integrated with the dish concentrator and condenser cover cooling. The dish concentrator increased the lower basin temperature to 85°C. The Charcoal and river sand increases the yield by 34.28 % and 25.71% by the conventional method. The cooling cover reduced the temperature of the condenser cover up to 8°C. The overall proposed system produced freshwater of 16.94  $\text{kg}/\text{m}^2$  [10]. *Arun & Sreekumar* compared the performance of the desalination system with different types of steel and glass covers in the parabolic trough collector with a sun tracking unit by focus line concentrator method. The results show that the maximum temperature reaches up to 75°C for stainless steel cover receivers and 103°C for glass cover receivers. The yield and efficiency of the system was increased to 2  $\text{L}/\text{m}^2$  and 12.74% respectively [11]. *Maliani et al.* proposed a new idea in designing and fabricating a tubular solar desalination hybrid with a two-axis solar tracking system. The result shows that the yield of the new still is 3.76  $\text{L}/\text{day}$ . The study concluded that the new tubular solar performance was higher than the compound parabolic concentrator and also reduced the cost of still by 7% [12]. In the tubular solar still fitted with the parabolic concentrator solar tracking device, *Mohamed et al.* studied the use of gravel as a suitable heat-storing material in solar desalination. The performance of the experiment was compared with and without sensible heat storage (gravel) elements in the system. This study found that the efficiency of the still and yield with gravel was 36.34% and 4.51  $\text{L}/\text{m}^2$ , respectively and without gravel, the efficiency and yield were 31.9% and 3.96  $\text{L}/\text{m}^2$  respectively [13]. *Sivakumar and Ganapathy Sundaram* studied the energy and exergy efficiency of the single slope solar still and concluded that the maximum energy destruction (3343.86  $\text{W}/\text{m}^2/\text{d}$ ) occurred in the basin liner (WI-WoD system) for the solar exergy input of 5813.35  $\text{W}/\text{m}^2$  in 1 cm water depth. Energy

efficiency can be improved by minimizing the exergy destruction and choosing the right material for the basin liner. [14]. *Farhad et al* theoretically studied the energy and efficiency of a solar desalination system comprising a humidification tower and a solar collector. The study concluded that a shorter humidification tower, an enormous tower, and a lower inlet air temperature were for the increase in total energy efficiency [15]. The bubble basin still gave better results compared to our conventional solar still the efficiency of the still was improved by more than 10%, and with humidification/dehumidification coupled with closed loop pulsating heat was produced yield up to 8.7 l/(day.m<sup>2</sup>)[16][17]. *Salek et al.* evaluated the energy and exergy of an atmospheric water generator integrated with the compound parabolic collector, and the mathematical model for the proposed system was developed using MAT LAB. The use of a storage tank extended the working hour of the system and increased the efficiency up to 400 L /month with a specific energy consumption of 3 kWh/L [18]. *Murugan et al.* carried out an extensive energy and exergy analysis on a stacked solar still and a single basin solar still to analyze its commercialization potential and the feasibility of the former. It is observed the maximum exergy loss is observed in the basin; however, in comparison, the exergy loss in the basin is higher for a single-basin solar still than a stacked solar still [19]. The energy and exergy analysis was a very important parameter while study about the receiver & collector in the solar desalination system, engines, cogeneration systems etc.,[20][21][22][23]. *Sajna Parimita Panigrahi et al.* investigated the unglazed transpired solar collectors (UTCs) for the heating application. They predicted the flow features random performance value by Monte Carlo simulation. The probability of an increase in efficiency is from 35% to 55.2%, and its increases the use UTCs in heating applications [24]. *Mohsen et al.* worked on solar cell cooling by Single-Walled Carbon Nano Tube (SWCNT)/water nanofluid. The parameters that the nanofluid made changes are the volume fraction of solid phase, solar radiation, ambient temperature and mass flow rate. The largest increase in the efficiency of the solar cell over the cell without cooling was 49.2%, 49.3 and 49.4% in the cases of employing water and the nanofluid at 0.5% and 1% concentrations, respectively [25]. *Kiran Naik et al.* developed a thermal model of a waste heat/solar heat-

driven membrane-based liquid desiccant regenerator. The performance of the membrane regenerator was predicted and analyzed by KNN-ML tool. It is observed that the use of a solar heater produces a high water extraction rate and better thermal performance compared to Waste Heat Recovery Exchanger (WHRE). Assessed the thermal performance of membrane-based liquid desiccant regenerator (MLDR) for different climatic conditions [26]. *Alireza et al.* developed a geothermal-based system with a Liquid Natural Gas (LNG) heat sink; it produced Heating load, cooling load, power, and freshwater. In this system, the best trade-off optimal points were identified by the LINMAP and TOPSIS methods. The overall efficiency and the total product cost are 29.15% and 1.512 \$/GJ, respectively. This system can produce 570.44 kW of power and 81.57 kg/s of potable water [27]. *Mahmoudan et al.* investigated the geothermal and solar-based multigeneration system integrated with a ThermoElectric Generator (TEG) Unit, The Multi-Objective Optimization Was Performed in the system. They concluded that the Energy efficiency, total unit cost of goods, and production rate of hydrogen are each 35.2%, 37.8%, and 1.9 kg/h, respectively. Also, they suggest removing the TEG unit in cold months for better performance [28]. *Kariman et al.* investigated energy and exergy analysis of industrial evaporation desalination systems integrated with Mechanical Vapor Recompression (MVR). They found that the more irreversibility occurred in the boiler chamber, work must be done on the boiler chamber in order to achieve greater energy efficiency. This system produced 60 L of fresh water per kilowatt-hour. It is much more economical in industrial aspects [29]. *Shoeibi et al.* made a detailed review of the evaporation improvement in solar still desalination using porous materials. The use of different materials as the porous medium will increase the rate of evaporation due to its high thermal conductivity. Activated carbon, Aluminium fins and Black steel wool increased the energy efficiency to 94.14%, 42.3% and 20.9%, respectively [30]. *Kariman et al.* investigated the Multi Effect Desalination (MED) system with a brine tank. A new model was developed, and the exergy analysis also carried for the model. The study concluded that the efficiency was increased from the range of 12–16 to 14–21.6 L/h for freshwater production; 30 - 40% of the output ratio was increased. The brine tank has the highest performance among other components, exergy efficiency of 82% [31].

*Jafari et al.* investigated on energy, economic, and environmental analysis of flat plate collectors for domestic application in Iran by Analytical Hierarchy Process (AHP). The payback period of investment (IPBP) was taken as the important parameter. They concluded that the yard in the centre of the country is the best place to install the system. Yard gains the maximum score of 26.5 out of 100. Tehran, Bandar Abbas, Rasht, and Tabriz got 24.4, 18.6, 15.9, and 14.6, respectively [32]. *Hoseinzadeh et al.* integrated the carbon dioxide power cycle with the geothermal energy source; it will give the energy to produce fresh water. Exergoeconomic analysis and optimization are studied, and as a result, 10% of the total cost rate was reduced in this method [33]. *Hoseinzadeh and Heyns* made advanced Energy, Exergy, and Environmental (3E) analyses and optimization of a coal-fired thermal power plant; in 400 MW power plant turbine system, condenser, pump, deaerator and heat exchangers and boiler, the amount of exergy destruction and exergetic efficiency of each component of the system is obtained by MATLAB software. They concluded that the highest rate of heat loss occurs at the feed water heater and the boiler with an amount of  $7.6 \times 10^4$  W and  $6.5 \times 10^7$  W. Therefore, analyzing their energy efficiency and environmental impacts can assist save in energy and ultimately lower emissions of pollutants including CO<sub>2</sub>, SO<sub>2</sub>, N<sub>2</sub>, and CO [34]. *Sohani et al.* developed an Artificial Neural Network (ANN) model to predict the hourly produced distillate and water temperature in the basin. They concluded that the Feed Forward (FF) and Radial Basis Function (RBF) are the best methods to predict it. The coefficient of determination was 0.963111 and 0.977057 for FF and RBF, respectively. The range of the daily water production projection inaccuracy is 2.41 to 5.84% per year [35]. *Dumka et al.* theoretical research was done using an ultrasonic fogger, cotton fabric, and typical solar still to analyze the system's energy, efficiency, and economics. A simple linear regression-based heat transfer model has been used to compare the CSS (Concentrated solar still) with the modified solar still (ultrasonic fogger and cotton cloth). As a result, the MSS (Modified Solar Still) has a 53.12% higher yield than CSS. The overall efficiency of the MSS was also 44.64% higher than CSS (Conventional Solar Still) [36]. *Abo-Elfadl et al.* evaluated the energy, efficiency, economics, and environmental impact of various condenser designs for a passive solar distiller.

The five different designs of condensers that were used are (i) glass plate condenser, GC (CSS), (ii) corrugated aluminium sheet heat sink condenser, CHS, (iii) aluminium heat sink condenser having vertical rectangular fins at its outer surfaces, RHS, (iv) aluminium heat sink condenser having pin fins at its outer surface, PHS, and (v) aluminium heat sink condenser having pin fins at its outer and inner surfaces, DPHS. PHS gives the maximum energy and exergy efficiency compared to CSS are 55.3% and 73.1%, respectively, and also suggests this model is best for CO<sub>2</sub> reduction benefits. DPHS model has Maximum production cost compared to PHS and CHS [37]. *Abd Elbar and Hassan* investigated the hybrid solar desalination with a solar panel to estimate the productivity, energy, exergy, exergoeconomic, and exergoenvironmental by water preheating and porous materials in Egypt's atmospheric condition. The result of preheating the saline water by 40%, 50%, and 60% gives the improvement in 10.4%, 15.5%, and 20.9% in yield, 8.2%, 13% and 20% in energy efficiency, and 26.86%, 33.51%, and 60.64% in exergy efficiency. Moreover, by using black steel wool fibres as insulation material, the performance was further increased to 17.8%, 13.7%, and 11.8% in yield, 13.58%, 9.73%, and 13.5% in energy efficiency, and 16.51%, 10.27%, and 32.45% in exergy efficiency respectively [38]. *Hassan et al.* investigated the energy, Exergy, exergoeconomic, enviro economic approaches and energy payback time of a parabolic trough collector (PTC) coupled with a single slope solar desalination system. Reading was taken in six models; CSS with or without PTC, CSS + Wire mesh with or without PTC, and CSS + Sand (SD) with or without PTC. The experiment was carried out in both summer and winter weather. The results show that the maximum yield occurs in CSS + SD + PTC likes 1.21% and 102.1% in summer and winter compared to CSS. Exergy efficiency improved to 216.6% and 325% compared to CSS in summer and winter, respectively [39]. The usage of active heating in the solar still, like parabolic trough collector and parabolic dish collector, increased the saline water temperature highly, resulting in the production of fresh water being also increased compared to conventional solar still. Compared to the passive system, the active system gave better performance in the heat utilization system [20, 40-44]. *Vahid et al.* explore an alternative approach to achieving a constant temperature of hot water from a solar water

**Table 1: Specifications of the experimental setup**

S.No	Dimensions	Measurements
1	Length of the Still	0.5 m
2	Width of the Still	0.5 m
3	Condenser Glass Angle	13°
4	Condenser Glass thickness	4 mm
5	Depth of water	30 mm
6	Dish Area	5.25 m <sup>2</sup>
7	Inner Insulation (Thermocol)	45 mm
8	Outer Insulation (Plywood)	18 mm

heater for process heat applications. Currently, auxiliary heating is used, but this incurs additional costs and greenhouse gas emissions. The proposed approach uses a phase change material in the hot water tank to moderate variations in outlet temperature. An experimentally-validated CFD model of a solar water heater with encapsulated paraffin wax phase change material was used, which delivered up to 1200 L of hot water at  $60\text{ }^{\circ}\text{C} \pm 2\text{ }^{\circ}\text{C}$  for more than 8 hours [45]. The windy conditions affected solar flux distribution, so the performance of the system was varied; this can be avoided by simulation techniques like FEM to find the best method or specification to find the solar flux distributions for any system [46, 47].

The literature found that the use of the concentrator will improve the performance of the solar still, and limited research works are carried out in the area of solar still with solar dish concentrators. In this regard, the present study proposes a new invention. The novel of this experimental work was a hybrid solar dish concentrator with the conventional solar still with four different aspects of with and without insulation and concentrator dish, with an objective to improve the performance of the solar still. The literature also found exergy analysis gives the idea about methods to improve the performance of the solar still. In this regard, the present research work is aimed at studying the energy and exergy analysis of the combination of solar still with solar dish concentrators. The performance of the solar still is studied with four different combinations i) Without Insulation-Without Dish (WoI-WoD), ii) With Insulation-Without Dish (WI-WoD), iii) Without Insulation-With Dish (WoI-WD), iv) With Insulation-With Dish (WI-WD). The performance of all the combinations and the energy and exergy analysis of the best performance mode (WI-WD) are studied and discussed in this research.

## EXPERIMENTAL SECTION

Single slope solar still was fabricated using a stainless steel plate with a thickness of 2 mm, 0.5m X 0.5m size. The inner side of the still was painted black colour for better absorption of solar radiation. The still is provided with two layers of insulation to avoid heat loss from the water inside the still. The first layer is made up of thermocol with a thickness of 45 mm; the second layer is made up of hardwood plywood with a thickness of 18 mm. A 4 mm thickness glass is used to cover the top of the still. The cover is placed at 13° inclination with horizontal (Latitude of Chennai) to maximize the yield. To avoid vapour leakage, the still and glass were sealed with window putty (chalk mixed with linseed oil). The water level inside the still was maintained at 3 cm height when the experiment was started in the morning, and no further water was added to the still. A dish with a size of 5.25 m<sup>2</sup> was used as a solar radiation concentrator to focus the solar radiation on the bottom of the still. Foil sheets were used as the reflective material in the dish. Solar still is faced towards the south to receive the maximum radiation. A collecting trough made of stainless steel was provided on the inner surface of the glass cover to collect the condensate water from the glass cover and pass it on to the collecting bottle. The specifications of the experimental setup are given in Table 1.

## Methodology

The experiment was conducted in Chennai (13° 8' 58.05" N, 80° 11' 32.38" E), Tamilnadu, India, on four different days during February and March 2020. In this experimental work, experiments were conducted on different days from 18<sup>th</sup> February to 12<sup>th</sup> March 2020. The readings were taken on four different days with different conditions; a) With Insulation-Without Dish (WI-WD), b) Without Insulation-Without Dish (WoI-WoD), c) Without Insulation-With Dish (WoI-WD), d) With Insulation-With Dish (WI-WD) and same average solar intensity

(Table 2) days with all the combinations proposed in this study were taken into consideration for the present analysis. The pictorial view of the four conditions is shown in Fig. 2, Fig. 3, Fig. 4, and Fig. 5. In the solar concentrator; the dish was manually tiled at a time interval of every 15 minutes to focus the solar radiation into solar still [11].

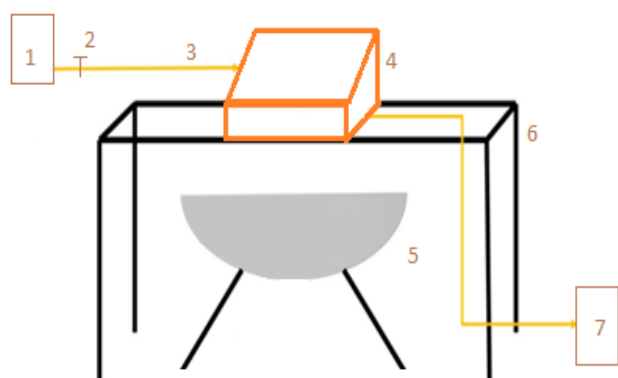
The solarimeter is used to measure the solar radiation falling on the still. The temperature at different locations and wind velocity are measured using Thermocouples and anemometers, respectively. A measuring

**Table 2: Average and cumulative radiations of the experiments with different conditions**

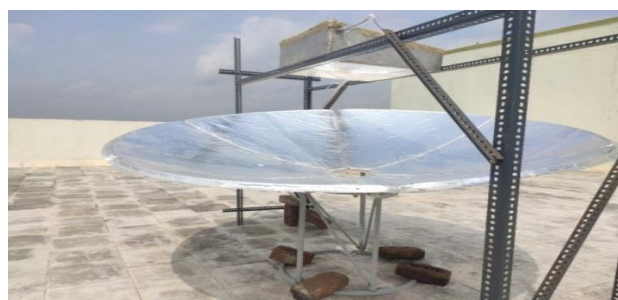
Date of Experiment in 2020	Condition	Notation	Average Radiation (W/m <sup>2</sup> )	Cumulative Radiation (W/m <sup>2</sup> .day)
21st February	With Insulation-Without Dish	WI-WoD	788.91	8678
5th March	Without Insulation-Without Dish	WoI-WoD	789.64	8686
6th March	Without Insulation-With Dish	WoI-WD	790.55	8696
11th March	With Insulation-With Dish	WI-WD	793.45	8728

**Table 3: Accuracy and range of the instruments used**

Instrument	Accuracy	Range
Thermocouples	$\pm 0.1^{\circ}\text{C}$	$-50-200^{\circ}\text{C}$
Solarimeter	$\pm 0.1 \text{ W/m}^2$	$0-2,000 \text{ W/m}^2$
Anemometer	$0.1\text{m/s}$	$0-30\text{m/s}$
Measuring jar	$\pm 1 \text{ mL}$	$0-250$



1. Saline water tank
2. Flow control valve
3. Pipelines
4. Single-slope solar still
5. Dish concentrator
6. Still, stand
7. Freshwater collector flask

**Fig. 1: Schematic diagram of experimental setup****Fig. 2: Solar still with insulation and without Dish (WI-WoD)****Fig. 3: Solar still without insulation and without dish (WoI-WoD)****Fig. 4: Solar still without insulation and with dish (WoI-WD)****Fig. 5: Condition 4 – Solar Still With Insulation-With Dish (WI-WD)**

jar is used to saline water poured into the solar still and the yield obtained from the still. The instruments used, their accuracy, and their range are given in Table 3.

## RESULTS AND DISCUSSION

### *Energy and exergy analysis of solar still–dish concentrator* *Energy analysis*

The energy utilized by the solar still and energy efficiency

of the overall system is found through the first law of thermodynamics. The daily efficiency  $\eta_{energy}$  of the solar still is calculated using Eqs (1)- (3) by adding up the hourly condensate output, multiplying by the latent heat of vaporization, and dividing by the daily total solar intensity, Direct and reflected by Dish, over the still solar area [14].

The hourly yield from 8 am to 7 pm can be added to get the daily yield (Mw).

*Energy Efficiency*

$$M_w = \left( \sum_{i=1}^{i=9} m_w \right) \quad (1)$$

Where,

$m_w$  = hourly yield in kg

$$\eta_{energy} = \frac{M_w \times L}{(A_s \times \sum_{t(s)}^I \times 3,600)} \quad (2)$$

$$L = 2.4935 \times 10^6 \times [1 - 9.4779 \times 10^{-4} T_w + 1.3131 \times 10^{-7} \times T_w^2 - 4.794 \times 10^{-9} \times T_w^3] \quad (3)$$

Where,

$A_s$  = Basin area of solar still (m<sup>2</sup>)

$A_{ap}$  = Dish area (m<sup>2</sup>)

$T_w$  = Water temperature (K)

*Exergy analysis*

Exergy analysis is derived from the second law of thermodynamics. The exergy of a thermodynamic system is part of the energy, which is the maximum useful work that can be obtained from the system at a given state in a specified Environment [14].

*Exergy efficiency*

According to the second law of thermodynamics the exergy analysis is derived in Eq. (4) and Eq. (5). Exergy efficiency was calculated by the ratio between exergy output and the exergy input.

$$\eta_{Ex} = 1 - \frac{E_{x_{dest}}}{E_{x_{sun}}} \quad (4)$$

$$\eta_{Exergy} = \frac{\frac{M_w \times L \left( 1 - \left( \frac{T_a}{T_s} \right) \right)}{3600}}{A_s \times \sum_{t(s)}^I \times \left( 1 + \frac{1}{3} \left( \frac{T_a}{T_s} \right)^4 - \frac{4}{3} \left( \frac{T_a}{T_s} \right) \right)} \quad (5)$$

Where

$T_a$  = Ambient temperature (K)

$T_s$  = Sun temperature (K)

**Exergy destruction of solar still–dish concentrator components**

The four major components of the present study were Basin liner, Saline water, glass cover, and dish concentrator. Their energy balance equations are provided below Equations (6), (10), (19) and (26).

**Exergy destruction of the basin**

The energy input to the solar still is the fraction of solar energy emitted by the sun  $\tau_{gl} \cdot \alpha_b \cdot \tau_w \cdot \tau_p \cdot E_{x_{sun}}$  that enters the solar still basin. The amount of energy actually utilized to heat the saline water is utilized exergy and is represented by ( $E_{x_w}$ ). In Equation (6), the remaining energy is lost from the still in different forms, and this is known as Exergy Destroyed ( $E_{x_{desb}}$ ) [14].

$$E_{x_{desb}} = (\tau_{gl} \cdot \alpha_b \cdot \tau_w \cdot \tau_p) E_{x_{sun}} + (\rho_d) E_{x_{sun}} - E_{x_w} - E_{x_{ins}} \quad (6)$$

Where

$\tau_{gl}$  = Transmittance of the glass cover.

$\tau_w$  = Transmittance of the saline water.

$\tau_p$  = Transmittance of the paint.

$\alpha_b$  = Absorptivity of the basin.

$\rho_d$  = Reflectivity of dish.

In Eq. (7), the exergy of the solar radiation on the solar still per unit area,  $E_{x_{sun}}$  (W/m<sup>2</sup>), is given as:

$$E_{x_{sun}} = I_{t(s)} \left[ 1 + \frac{1}{3} \left( \frac{T_a}{T_s} \right)^4 - \frac{4}{3} \left( \frac{T_a}{T_s} \right) \right] \quad (7)$$

$T_s$  = temperature of the sun (5777 K).

$T_a$  = Ambient Air Temperature

$$E_{x_w} = \square_{cb-w} (T_b - T_w) \left( 1 - \frac{T_a}{T_b} \right) \quad (8)$$

Where

$\square_{cb-w}$  = Convective heat transfer coefficient between the basin and saline water (W/m<sup>2</sup>K).

$T_b$  = temperature of the basin (K)

$T_w$  = temperature of the saline water (K).

$$E_{x_{ins}} = \square_b (T_b - T_a) \left( 1 - \frac{T_a}{T_b} \right) \quad (9)$$

$\square_b$  = Overall heat transfer coefficient between basin liner and atmosphere ( $\text{W/m}^2 \text{ K}$ ).

### Exergy destruction of saline water

The total of the fractional solar Exergy serves as the exergy input for the saline water ( $\tau_{gl} \cdot \alpha_w \cdot E_{Xsun}$ ) absorbed by the water, and the dish's reflection is used to increase the temperature of the salt water ( $\rho_d \cdot E_{Xsun}$ ). It is used as the Exergy involved in the heat transfer between the surface of the salt water and the interior of the glass cover ( $E_{X_{t,w-gl}}$ ), and the remaining is destroyed ( $E_{X_{des,w}}$ )

$$E_{X_{des,w}} = (\tau_{gl} \cdot \alpha_w) E_{Xsun} + (\rho_d) E_{Xsun} - E_{X_{t,w-gl}} \quad (10)$$

Where

$\tau_{gl}$  - Transmittance of the glass cover.

$\alpha_w$  - Absorptivity of saline water.

$\rho_d$  - Reflectivity of Dish

$E_{X_{t,w-gl}}$  It is calculated as follows.

$$E_{X_{t,w-gl}} = E_{X_{eva,w-gl}} + E_{X_{con,w-gl}} + E_{X_{rad,w-gl}} \quad (11)$$

Equation (12), Equation (13) and Equation (15) are the Exergy associated with the heat transfer through evaporation, convection, and radiation between the saline water surface and the inner side of the glass cover.

$$E_{X_{eva,w-gl}} = \square_{eva,w-gl} (T_w - T_{gi}) \left( 1 - \frac{T_a}{T_w} \right) \quad (12)$$

Where

$\square_{eva,w-gl}$  = Evaporative heat transfer coefficient between saline water and the inner side of the glass cover ( $\text{W/m}^2 \text{ K}$ )

$T_{gi}$  = Glass inner surface temperature (K).

$$h_{eva,w-gl} = 0.016273 h_{c,w-gl} \frac{P_w - P_{gi}}{T_w - T_{gi}} \quad (13)$$

Where

$P_w$  = Partial pressures of water vapour ( $\text{N/m}^2$ )

$P_{gi}$  = Partial pressures of inner glass surface temperatures within the still, which are given by as:

$$P(T) = \exp \left[ 25.317 - \frac{5144}{T} \right] \quad (14)$$

$$E_{X_{c,w-gl}} = \square_{c,w-gl} (T_w - T_{gi}) \left( 1 - \frac{T_a}{T_w} \right) \quad (15)$$

Where

$h_{c,w-gl}$  = Convective heat transfer coefficient between saline water and the inner side of the glass cover ( $\text{W/m}^2 \text{ K}$ ).

$$h_{c,w-gl} = 0.884 \left[ T_w - T_{gi} + \frac{(P_w - P_{gi}) T_w}{26890 - P_w} \right]^{1/3} \quad (16)$$

$$E_{X_{r,w-gl}} = h_{r,w-gl} (T_w - T_{gi}) \left[ 1 + \frac{1}{3} \left( \frac{T_a}{T_w} \right)^4 - \frac{4}{3} \left( \frac{T_a}{T_w} \right) \right] \quad (17)$$

Where,

$h_{r,w-gl}$  = Radiative heat transfer coefficient between saline water and the inner side of the glass cover ( $\text{W/m}^2 \text{ K}$ )

$$h_{r,w-gl} = \epsilon_{eff} \sigma (T_w^2 + T_{gi}^2) (T_w + T_{gi}) \quad (18)$$

Where,

$\epsilon_{eff}$  = Effective emissivity is taken as 0.82.

$\sigma$  = Stefan – Boltzmann constant is taken as  $5.67 \times 10^{-8} \text{ W/m}^2 \text{ K}^4$ .

### Exergy destruction of the glass cover

In Equation (19), the exergy input for the glass cover is the sum of the fraction of solar exergy ( $\alpha_g E_{Xsun}$ ) absorbed by the glass cover and the Exergy associated with the heat transfer between the saline water surface and the inner side of the glass cover ( $E_{X_{t,w-gl}}$ ). A part of this Exergy is lost to the atmosphere by convection and radiation heat transfer, and the remaining is destroyed  $E_{X_{des,gl}}$ .

$$E_{X_{des,gl}} = \alpha_g E_{Xsun} + E_{X_{t,w-gl}} - E_{X_{t,gl-a}} \quad (19)$$

Where

$\alpha_g$  = Absorptivity of the glass cover

$E_{X_{t,gl-a}}$  is calculated as follows.

$$E_{X_{t,gl-a}} = E_{X_{c,gl-a}} + E_{X_{r,gl-a}} \quad (20)$$

$$E_{X_{c,gl-a}} = h_{c,gl-a} (T_{go} - T_a) \left( 1 - \frac{T_a}{T_{go}} \right) \quad (21)$$

$$h_{c,gl-a} = 5.7 + 3.8V \quad (22)$$

Where

$h_{c,gl-a}$  = Convective heat transfer coefficient between the glass cover and atmosphere ( $\text{W/m}^2 \text{ K}$ )

$T_{go}$  = Outer glass temperature (K).

$V$  = wind speed in m/s.

$$E_{X_{r,gl-a}} = h_{r,gl-a} (T_{go} - T_a) \left[ 1 + \frac{1}{3} \left( \frac{T_a}{T_{go}} \right)^4 - \frac{4}{3} \left( \frac{T_a}{T_{go}} \right) \right] \quad (23)$$

Where

$\square_{r,gl-a}$  = Radiative heat transfer coefficient between the glass cover and atmosphere ( $\text{W/m}^2 \text{ K}$ )

Table 4: Design constants used for analysis

S. No.	Parameter	Value
1	Absorptivity of glass cover ( $\alpha_g$ )	0.05
2	Absorptivity of basin liner ( $\alpha_b$ )	0.9
3	Absorptivity of water ( $\alpha_w$ )	0.05
4	Absorptivity of the dish ( $\alpha_d$ )	0.20
5	Transmissivity of glass cover ( $\tau_g$ )	0.9
6	Transmissivity of water ( $\tau_w$ )	0.95
7	Reflectivity of the glass cover ( $\gamma$ )	0.05
8	Effective emissivity( $\varepsilon_{eff}$ )	0.82
9	The optical efficiency of a foil sheet ( $\eta_{opt}$ )	80%
10	Reflectivity of the dish ( $\rho_d$ )	0.80
11	Thermal conductivity of Insulating material ( $K_{ins}$ )	0.015 W/m K
12	Heat transfer coefficient between basin liner and water surface ( $\square_w$ )	135 W/m <sup>2</sup> K
13	Overall heat transfer coefficient between basin liner and atmosphere ( $\square_b$ )	14 W/m <sup>2</sup> K
14	Stefan—Boltzmann constant ( $\sigma$ )	$5.67 \times 10^{-8}$ W/m <sup>2</sup> K <sup>4</sup>

$$h_{r,gl-a} = \frac{\varepsilon_{eff} \sigma (T_{go}^4 - T_{sky}^4)}{T_{go} - T_{sky}} \quad (24)$$

$$T_{sky} = 0.0552 T_a^{1/5} \quad (25)$$

Where

$T_{sky}$  = Sky temperature (K)

#### Exergy destruction of dish

In Equation (27), the exergy input for the dish is the sum of the fraction of the ( $\alpha_d \cdot E_{x_{sun}}$ ) solar energy absorbed by the dish. The reflectivity energy of the dish is based on the ( $\eta_{opt}$ ) optical efficiency of the surface. A part of this Exergy is lost to the atmosphere by convection and radiation heat transfer, and the remaining is destroyed ( $E_{x_{des.d}}$ ).

$$E_{x_d} = \eta_{opt} I_b A_{ap} \left( 1 + \frac{1}{3} \left( \frac{T_a}{T_s} \right)^4 - \frac{4}{3} \left( \frac{T_a}{T_s} \right) \right) \quad (26)$$

$$E_{x_{des.d}} = (\alpha_d \cdot E_{x_{sun}}) - E_{x_d} \quad (27)$$

Where

$T_a$  = temperature of the atmosphere outside the solar still (K)

$\eta_{opt}$ . = Optical efficiency is taken as 80%.

$I_b$  = Beam radiation.

$A_{ap}$  = Area of the Dish (5.25 m<sup>2</sup>).

Table 4 listed out the design constants used in this study.

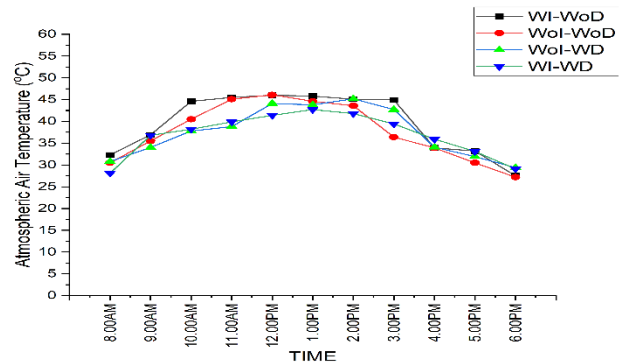
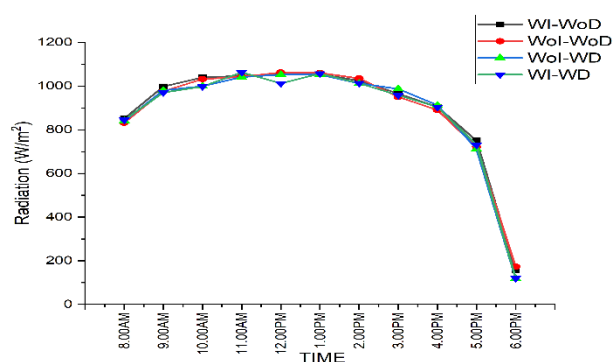


Fig. 6: Variation of atmospheric air temperature with time for different combinations

#### Performance of solar still–dish concentrator components

##### Atmospheric air temperature:

The energy and exergy analysis of single slope solar still with solar dish concentrator has been carried out with four different combinations in this study. Fig. 6 shows the variation of atmospheric air temperature with time for all four combinations. The atmospheric temperature will change the outer temperature of the still glass cover and insulation outer surface, which will affect the solar still yield [2, 18, 37]. The study found that the same atmospheric air temperature is observed in both morning and afternoon for all four combinations. A small variation in atmospheric air temperature is observed between the combinations



**Fig. 7: Variation of solar intensity with local time for different combinations**

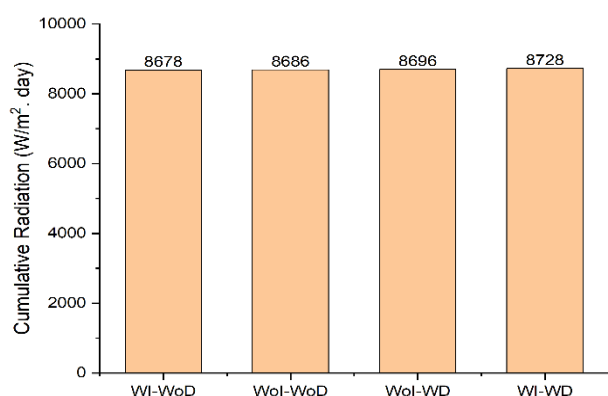


**Fig. 8: Cumulative daily solar intensity for different combinations**

during the afternoon. The maximum atmospheric air temperature difference among all the combinations is 4.4°C at 12 noon, and a 1.5°C temperature difference is observed at 4 PM. This shows that the influence of atmospheric air temperature on the difference in still yield between different combinations in this study is negligible.

### **The intensity of solar radiation**

The saline water temperature inside the still mainly depends on the intensity of the solar radiation falling on the still [2,19, 39]. Fig.7 shows the hourly variation of solar radiation intensity falling on the still with time for the four combinations. The incident solar radiation intensity increased up to 1.00 PM in the morning and started decreasing thereafter up to evening. The same trend is observed for all four combinations in this study. The maximum radiation intensity is observed as 1062, 1056, 1052, and 1070 W/m<sup>2</sup> for the experiments conducted with WoI-WoD,

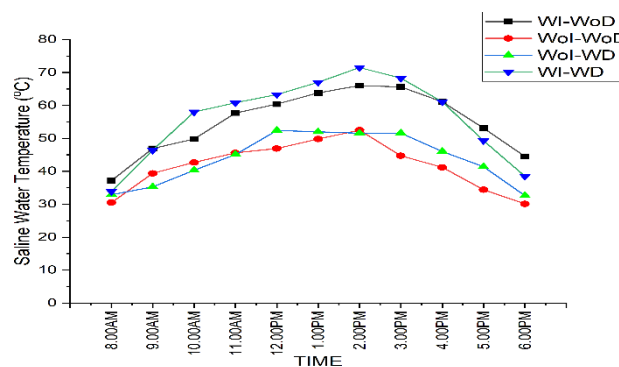


**Fig. 9: Variation of saline water temperature with time**

WI-WoD, WoI-WD and WI-WD combinations, respectively. The cumulative daily solar intensity falling on the still is shown in Fig. 8 for all four combinations. The cumulative solar intensity is 8686, 8678, 8696, and 8728 W/m<sup>2</sup>.day for WoI-WoD, WI-WoD, WoI-WD and WI-WD combinations, respectively. Very small variation in cumulative daily solar intensity is observed between all the combinations. The maximum cumulative solar intensity variation observed between all the combinations is 50 W/m<sup>2</sup>.day. The hourly variation of solar intensity and cumulative daily solar intensity for all four combinations shows that the influence of solar intensity on the difference in still yield between different combinations in this study is negligible.

### **Saline water temperature**

Fig. 9 shows the saline water temperature with time for different combinations in this study. The water temperature is low in the WoI-WoD combination, particularly in the afternoon, due to the non-availability of insulation over the still, which leads to higher heat loss from the still to atmospheric air. Compared to WoI-WoD, the water temperature is higher in

WoI-WD combination from 11 AM onwards; this is due to additional heat input to the still from the dish concentrator.

In the case of WI-WoD and WI-WD, up to 3 PM, the still water temperature is higher in the case of WI-WD as compared to WI-WoD, but after 3 PM, this condition is reversed. The water temperature for WI-WoD is higher than WI-WD. This is due to heat loss from the bottom of the still being higher than the additional heat observed, reflected by the dish concentrator, by the WI-WD combination. The maximum water temperature of 73.5°C

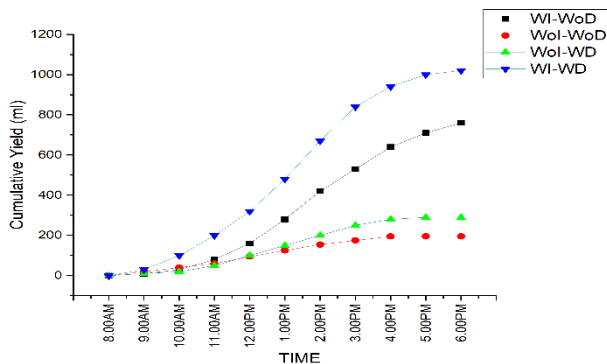


Fig. 10: Variation of cumulative yield with time for different combinations

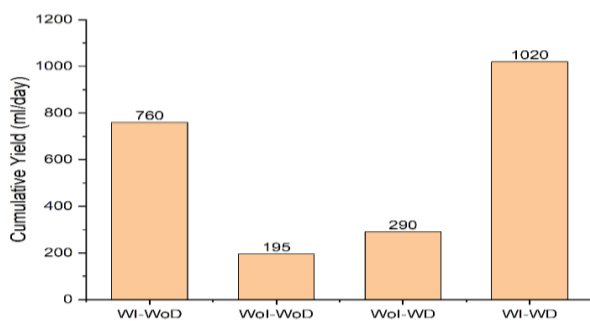


Fig. 11: Cumulative yield per day with different combinations

is observed in the WI-WD combination at 2 PM. The use of a dish concentrator increased the saline water temperature both in the case of WI-WD and WoI-WD because insulation supported to reduce the heat loss from the still to atmospheric air. But the increase in temperature is higher for WI-WD as compared to WoI-WD.

#### Mass of water evaporated

The hourly cumulative yield and total cumulative yield obtained from all the combinations in this study are shown in Fig. 10 and Fig. 11, respectively. For all the combinations, the hourly cumulative yield increased continuously from morning to evening. The variation of cumulative yield between the combinations is minimal up to the morning.

11 AM After that, there is an increase in the yield for both WI-WoD and WI-WD compared to the other two combinations. The solar still with the combination WI-WoD is studied by several researchers, and results are reported in the literature. The yield obtained from (WI-WoD) combination in this study is 760 mL for a 0.25m area of solar still. Similar yield is found in the literature [2,3,30,48].

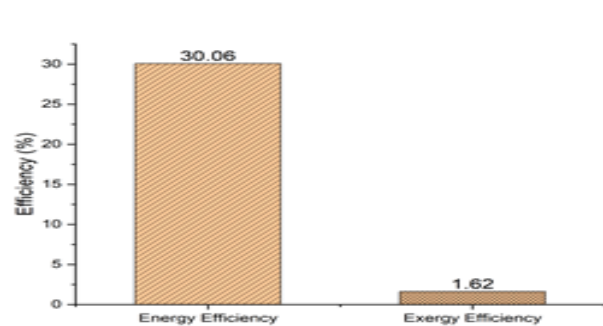


Fig. 12: Energy and exergy efficiency of the combination WI-WD

The daily cumulative yield obtained from the combinations WoI-WoD, WI-WoD, WoI-WD and WI-WD is 195, 760, 290, and 1020 mL, respectively, for 0.25m<sup>2</sup> area of the solar still. Providing insulation decreased the heat loss from the still to atmospheric air and increased the yield from 195 mL to 760 mL in WI-WoD as compared to WoI-WoD. The yield from the WI-WD combination is very high compared to another combination because the dish concentrator focused additional solar radiation into the still, increased the saline water temperature, and increased the cumulative yield. Within insulation combinations, the cumulative yield is increased from 760 mL/day in WI-WoD to 1020 mL/day in WI-WD. In the case of WI-WD, the bottom of the still is not insulated to observe the heat from the dish concentrator and pass on it into the saline water; because of this, after 5 PM, the hourly yield from WI-WoD is higher than WI-WD in this study. Proper insulation increased the daily yield by 74.34% compared to without insulation. Even though the bottom of the still is not insulated in the WI-WD combination, it increased the yield by 25.49% as compared to WI-WoD. Solar still with dish concentrator and proper insulation at the bottom of the still will further increase the daily yield.

#### Energy and exergy analysis

Energy and Exergy efficiency are the two significant elements of the thermal systems and give the idea about the performance of any system. The exergy efficiency and exergy destruction of the components contribute to the losses in the overall system will support taking measures for minimizing the losses and further improving the performance of the overall system.

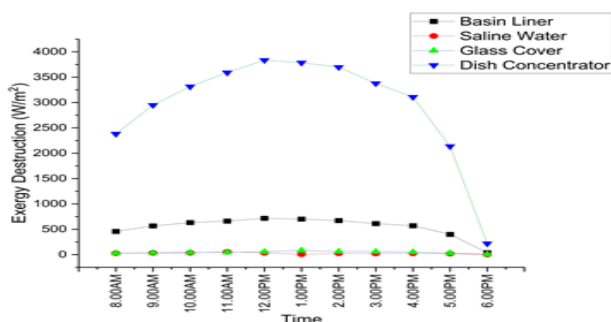


Fig. 13: Hourly Exergy Destruction of basin liner, saline water, glass cover & dish concentrator

Since the saline water temperature and water yield are higher in the combination WI-WD as compared to other combinations in this study, the energy and exergy analysis is carried out with WI-WD combinations and discussed in this section. Fig. 12 shows the energy and exergy efficiency of the combination WI-WD. The energy and exergy efficiencies are 30.06 and 1.6%, respectively. The energy and exergy efficiency are higher than the values reported in the literature [14,15,31,36]. The use of a dish concentrator increased the energy efficiency, exergy efficiency and performance of the still by increasing the yield. The energy and exergy efficiency of the still will be further increased by optimizing the water depth, use of phase change materials and different techniques used to improve the still yield [49-51].

The instantaneous exergy destruction has been calculated for the components of the solar still: basin liner, saline water, glass cover, and dish concentrator. Fig. 13 shows the hourly variation of exergy destruction of various components. The maximum hourly exergy destruction in basin liner, saline water, glass cover and dish concentrator are 716.53, 53.82, 82.99 and 3836 W/m<sup>2</sup>, respectively, for the WI-WD combination. A similar order of exergy destruction is found in the literature [14]. It is observed that the largest exergy destruction takes place in the basin liner compared to saline water and glass cover in the still components. This may be due to the high-temperature difference between the basin liner and atmospheric air. Due to the very high temperature in the dish concentrator, the exergy destruction in the dish concentrator is very high as compared to still components. The reduction in exergy destruction of basin liners by proper basin material and efficient methods to focus solar radiation from the dish concentrator will improve the exergy efficiency and overall performance of the still.

## CONCLUSION

In this study, the performance of the single slope solar still with dish concentrator is studied using an energy and exergy approach in terms of ambient air temperature, daily cumulative solar intensity, saline water temperature, hourly yield and cumulative daily yield. The solar flux distribution inside the system varied between 8678 and 8728 W/m<sup>2</sup>.day. The findings from the study are summarized below.

- The WI-WD combination produced maximum saline water temperature as compared to other combinations. The maximum water temperature of 73.5°C is observed in the WI-WD combination at 2 PM. Up to 3 PM, the still water temperature is higher in the case of WI-WD as compared to WI-WoD, but after 3 pm, the water temperature for WI-WoD is higher than WI-WD.
- The daily cumulative yield obtained from the combinations WoI-WoD, WI-WoD, WoI-WD and WI-WD is 195, 760, 290, and 1020 mL for 0.25 m<sup>2</sup> area, respectively. Proper insulation increased the daily yield by 74.34% compared to without insulation. The WI-WD combination increased the yield by 25.49% as compared to
- WI-WoD. Still, a dish concentrator and proper insulation at the bottom of the still will further increase the daily yield.
- The energy and exergy efficiencies are 30.06 and 1.6%, respectively, for the WI-WD combination, which is higher than conventional solar still without a dish concentrator.
- The largest exergy destruction is observed in the dish concentrator. Among the still components, the basin liner produced higher exergy destruction compared to saline water and glass cover. The maximum hourly exergy destruction in the basin liner, saline water, glass cover and dish concentrator are observed as 716.53, 53.82, 82.99 and 3836 W/m<sup>2</sup>, respectively, for the WI-WD combination.
- Solar still – Dish concentrator combination with phase change materials, Lower water level depth, proper material for basin liner and sun tracking system will support to improve the performance of the still.

## Nomenclature

$M_w$	Mass of saline water (kg)
$M_b$	Mass of the basin (kg)
$m$	Hourly distillate yield (kg)
$C_{p_w}$	Specific heat of water (J /kg K)
$C_{p_b}$	Specific heat of basin (J /kg K)

$C_{pg}$	Specific heat of glass (J /kg K)	$\square_{r,w-gl}$	Radiative heat transfer coefficient between saline water and glass cover (W / m <sup>2</sup> K)
$K_{ins}$	Thermal conductivity of insulation material (W/m <sup>2</sup> K)	$\square_{c,gl-a}$	Convective heat transfer coefficient between the glass cover and atmosphere (W / m <sup>2</sup> K)
$K_{wood}$	Thermal conductivity of wood (W/m <sup>2</sup> K)	$\square_{r,gl-a}$	Radiative heat transfer coefficient between the glass cover and atmosphere (W / m <sup>2</sup> K)
$L_{ins}$	Thickness of insulation (m)	$\alpha_g$	Absorptivity of the glass cover
$L_{wood}$	Thickness of wood material (m)	$\alpha_b$	Absorptivity of basin liner
$\square_{fg}$	Latent heat of vaporization (J /kg)	$\alpha_w$	Absorptivity of water
$A_s$	Basin area of solar still (m <sup>2</sup> )	$\alpha_d$	Absorptivity of dish
$A_{ap}$	Dish area (m <sup>2</sup> )	$\tau_g$	Transmissivity of the glass cover
$I_t$	Hourly incident solar radiation (W /m <sup>2</sup> )	$\tau_w$	Transmissivity of water
$T_a$	Ambient air temperature (K)	$\gamma$	Reflectivity of the glass cover
$T_w$	Water temperature (K)	$\rho_d$	Reflectivity of the dish
$T_b$	Basin temperature (K)	$\varepsilon_{eff}$	Effective emissivity
$T_{gi}$	Inner glass temperature (K)	$\eta_{opt}$	The optical efficiency of a foil sheet
$T_{go}$	Outer glass temperature (K)	$\sigma$	Stefan – Boltzmann constant
$T_{sky}$	Sky temperature (K)		
$E_{x_{des,b}}$	Exergy destruction from basin liner (W / m <sup>2</sup> )		
$E_{x_{des,w}}$	Exergy destruction from saline water (W / m <sup>2</sup> )		
$E_{x_{des,gl}}$	Exergy destruction from glass cover (W / m <sup>2</sup> )		
$E_{x_{ins}}$	Exergy loss through insulation (W / m <sup>2</sup> )		
$E_{x_w}$	Exergy utilized to heat saline water (W / m <sup>2</sup> )		
$E_{x_{t,w-gl}}$	Total Exergy associated with saline water and glass cover (W / m <sup>2</sup> )		
$E_{x_{e,w-gl}}$	Exergy associated with saline water and glass cover through evaporation (W / m <sup>2</sup> )		
$E_{x_{c,w-gl}}$	Exergy associated with saline water and glass cover through convection (W / m <sup>2</sup> )		
$E_{x_{r,w-gl}}$	Exergy associated with saline water and glass cover through radiation (W / m <sup>2</sup> )		
$E_{x_{t,gl-a}}$	Total Exergy associated with glass cover and atmosphere (W / m <sup>2</sup> )		
$E_{x_{c,gl-a}}$	Exergy associated with glass cover and atmosphere through convection (W / m <sup>2</sup> )		
$E_{x_{r,gl-a}}$	Exergy associated with glass cover and atmosphere through radiation (W / m <sup>2</sup> )		
$\square_{c,wood-a}$	Convective heat transfer between wood and atmosphere (W / m <sup>2</sup> K)		
$\square_{c,b-w}$	Convective heat transfer between basin and water (W / m <sup>2</sup> K)		
$\square_b$	Overall heat transfer between basin and atmosphere (W / m <sup>2</sup> K)		
$\square_{eva,w-gl}$	Evaporative heat transfer coefficient between saline water and glass cover (W / m <sup>2</sup> K)		
$\square_{c,w-gl}$	Convective heat transfer coefficient between saline water and glass cover (W / m <sup>2</sup> K)		

Received : Oct. 26, 2022 ; Accepted : Apr.24, 2023

## REFERENCE

- [1] Norouzi N., Bozorgian A., Dehghani M.A., [Best Option of Investment in Renewable Energy: A Multicriteria Decision-Making Analysis for Iranian Energy Industry](#), *J. Environ. Assess. Policy Manag.*, **22**(1–2): (2020).
- [2] Panchal H. N., Patel S., [An Extensive Review on Different Design and Climatic Parameters to Increase Distillate Output of Solar Still](#), *Renew. Sustain. Energy Rev.*, **69**: 750–758 (2017) .
- [3] Yuvaraj M., Sudharani R., R Suresh., Kumar A., Raghuram K. S., kuila S., Influence of Nano-Coating on the Productivity of a Double Slope Solar Still, *Mater. Today Proc.*, **69**: 744–748 (2022).
- [4] Kabeel A. E., Elkelawy M., Alm El Din H., Alghrubah A., [Investigation of Exergy and Yield of a Passive Solar Water Desalination System with a Parabolic Concentrator Incorporated with Latent Heat Storage Medium](#), *Energy Convers. Manag.*, **145**: 10–19 (2017).
- [5] Hamed O.A., Kosaka H., Bamardouf K. H., Al-Shail K., Al-Ghamdi A. S., [Concentrating Solar Power for Seawater Thermal Desalination](#), *Desalination*, **396**: 70–78 (2016).
- [6] Rafiei A., Loni R., Mahadzir S. B., G Najafi., Pavlovic S., Bellos E., [Solar Desalination System with a focal Point Concentrator Using Different Nanofluids](#), *Appl. Therm. Eng.*, **174**: (2020).

- [7] Omara Z. M., Eltawil M. A., [Hybrid of Solar Dish Concentrator, New Boiler and Simple Solar Collector for Brackish Water Desalination](#), *Desalination*, **326**: 62–68 (2013).
- [8] Abubakkar A., Selvakumar P., Rajagopal T., Tamilvanan A., [Development of Concentrating Dish and Solar Still Assembly for Sea Water Desalination](#), *Mater. Today Proc.*, **45**: 974–980 (2021).
- [9] Riffat S., Mayere A., [Performance Evaluation of V-Trough Solar Concentrator for Water Desalination Applications](#), *Appl. Therm. Eng.*, **50**(1): 234–244 (2013).
- [10] Srithar K., Rajaseenivasan T., Karthik N., Periyannan M., Gowtham M., [Stand Alone Triple Basin Solar Desalination System with Cover Cooling and Parabolic Dish Concentrator](#), *Renew. Energy*, **90**: 157–165 (2016).
- [11] Arun C.A., Sreekumar P.C., [Modeling and Performance Evaluation of Parabolic trough Solar Collector Desalination System](#), *Mater. Today Proc.*, **5** (1): 780–788 (2018).
- [12] Maliani O.D., Bekkaoui A., Baali E.H., Guissi K., El Fellah Y., Errais R., [Investigation on Novel Design of Solar Still Coupled with Two Axis Solar Tracking System](#), *Appl. Therm. Eng.*, **172**: (2020).
- [13] Elashmawy M., [Improving the Performance of a Parabolic Concentrator Solar Tracking-Tubular Solar Still \(PCST-TSS\) Using Gravel as a Sensible Heat Storage Material](#), *Desalination*, **473**: (2020).
- [14] Vaithilingam S., Esakkimuthu G.S., [Energy and Exergy Analysis of Single Slope Passive Solar Still: An Experimental Investigation](#), *Desalin. Water Treat.*, **55**(6): 1433–1444 (2014).
- [15] Nematollahi F., Rahimi A., Gheinani T.T., [Experimental and Theoretical Energy and Exergy Analysis for a Solar Desalination System](#), *Desalination*, **317**: 23–31 (2013).
- [16] Aref L., Fallahzadeh R., Madadi Avargani V., [An Experimental Investigation on a Portable Bubble Basin Humidification/Dehumidification Desalination Unit Utilizing a Closed-Loop Pulsating Heat Pipe](#), *Energy Convers. Manag.*, **228**(2020): 113694 (2021).
- [17] Fallahzadeh R., Aref L., Madadi Avargani V., Gholamirjenaki N., [An Experimental Investigation on the Performance of a New Portable Active Bubble Basin Solar Still](#), *Appl. Therm. Eng.*, **181**: 115918 (2020).
- [18] Salek F., Eshghi H., Zamen M., Ahmadi M.H., [Energy and Exergy Analysis of an Atmospheric Water Generator Integrated with the Compound Parabolic Collector with Storage Tank in Various Climates](#), *Energy Reports*, **8**: 2401–2412 (2022).
- [19] Murugan D.K., Subramani S., Thirugnanasambantham A., Munuswamy K., [Thermo-Economic Comparison of Single Basin and Stacked Solar Still Configurations](#), *Environ. Sci. Pollut. Res.*, **29**(47): 71650–71664 (2022).
- [20] Bahrami M., Madadi Avargani V., Bonyadi M., [Comprehensive Experimental and Theoretical Study of a Novel Still Coupled to a Solar Dish Concentrator](#), *Appl. Therm. Eng.*, **151**: 77–89 (2019).
- [21] Madadi V., Tavakoli T., Rahimi A., [Estimation of Heat Loss from a Cylindrical Cavity Receiver Based on Simultaneous Energy and Exergy Analyses](#), *J. Non-Equilibrium Thermodyn.*, **40**(1): 49–61 (2015).
- [22] Norouzi N., Ebadi A.G., Bozorgian A.R., Hoseyni S.J., Vessally E., [Energy and Exergy Analysis of Internal Combustion Engine Performance of Spark Ignition for Gasoline, Methane, and Hydrogen Fuels](#), *Iran. J. Chem. Chem. Eng.(IJCCE)*, **40**(6):1909–1930 (2021).
- [23] Nourozi N., Ebadi A. G., Bozorgian A., Hoseyni S. J., Vessally E., [Cogeneration System of Power, Cooling, and Hydrogen from Geothermal Energy: An Exergy Approach](#), *Iran. J. Chem. Chem. Eng. (IJCCE)*, **41**(2): 706–721 (2022).
- [24] S.C.A., Sajna M.A., Parimita P., Maharana S.K., Rajashekaraiah T., Gopalashetty R., Sharifpur M., Ahmadi M.H., [“Flat Unglazed Transpired Solar Collector](#), *MDPI*, **15**(23): (2022).
- [25] Sharifpur M., Ahmadi M.H., Rungamornrat J., Malek Mohsen F., [Thermal Management of Solar Photovoltaic Cell by Using Single Walled Carbon Nanotube \(SWCNT\)/Water: Numerical Simulation and Sensitivity Analysis](#), *Sustain.*, **14**(18): (2022).
- [26] Kiran Naik B., Chinthala M., Patel S., Ramesh P., [Performance Assessment of Waste Heat/Solar Driven Membrane-Based Simultaneous Desalination and Liquid Desiccant Regeneration System Using a Thermal Model and KNN Machine Learning Tool](#), *Desalination*, **505**: 114980 (2021).
- [27] Mahmoudan A., Samadof P., Hosseinzadeh S., Garcia D.A., [A Multigeneration Cascade System Using Ground-Source Energy with Cold Recovery: 3E Analyses and Multi-Objective Optimization](#), *Energy*, **233**: 121185 (2021).

- [28] Mahmoudan A., Esmaeilion F., Hoseinzadeh S., Soltani M., Ahmadi P., Rosen M., [A Geothermal and Solar-Based Multigeneration System Integrated with a TEG Unit: Development, 3E Analyses, and Multi-Objective Optimization](#), *Appl. Energy*, **308**: (2021).
- [29] Kariman H., Hoseinzadeh S., Heyns P.S., [Energetic and Exergetic Analysis of Evaporation Desalination System Integrated with Mechanical Vapor Recompression Circulation](#), *Case Studies in Thermal Engineering*, **16**: (2019)
- [30] Shoeibi S. *et al.*, [A Review on Evaporation Improvement of Solar Still Desalination using Porous Material](#), *Int. Commun. Heat Mass Transf.*, **138**: 106387, (2022).
- [31] Kariman H., Hoseinzadeh S., Heyns S., Sohani A., [Modeling and Exergy Analysis of Domestic Med Desalination with Brine Tank](#), *Desalin. Water Treat.*, **197**: 1–13 (2020).
- [32] Jafari S., Sohani A., Hoseinzadeh S., Pourfayaz F., [The 3E Optimal Location Assessment of Flat- Plate Solar Collectors for Domestic Applications in Iran](#), *Energies*, **15**(10): 1–17 (2022).
- [33] Hoseinzadeh S., Yargholi R., Kariman H., Heyns P.S., [Exergoeconomic Analysis and Optimization of Reverse Osmosis Desalination Integrated with Geothermal Energy](#), *Environ. Prog. Sustain. Energy*, **39**(5): 1–9 (2020).
- [34] Hoseinzadeh S., Heyns P.S., [Advanced Energy, Exergy, and Environmental \(3E\) Analyses and Optimization of a Coal-Fired 400 MW Thermal Power Plant](#), *J. Energy Resour. Technol. Trans. ASME*, **143**(8): 1–9 (2021).
- [35] Sohani A., Hoseinzadeh S., Samiezadeh S., Verhaert I., [Machine Learning Prediction Approach for Dynamic Performance Modeling of an Enhanced Solar Still Desalination System](#), *J. Therm. Anal. Calorim.*, **147**(5): 3919–3930 (2022).
- [36] Dumka P., Jain A., Mishra D.R., [Energy, Exergy, and Economic Analysis of Single Slope Conventional Solar still Augmented with an Ultrasonic Fogger and a Cotton Cloth](#), *Undefined*, **30**: (2020).
- [37] Abo-Elfadl S., Yousef M.S., Hassan H., [Energy, Exergy, Economic and Environmental Assessment of Using Different Passive Condenser Designs of Solar Distiller](#), *Process Saf. Environ. Prot.*, **148**: 302–312 (2021).
- [38] Abd Elbar A.R., Hassan H., [Energy, Exergy and Environmental Assessment of Solar Still with Solar Panel Enhanced by Porous Material and Saline Water Preheating](#), *J. Clean. Prod.*, **277**: (2020).
- [39] Hassan H., Yousef M. S., Fathy M., Ahmed M.S., [Assessment of Parabolic trough Solar Collector Assisted Solar Still at Various Saline Water Mediums via Energy, Exergy, Exergoeconomic, and Enviroeconomic Approaches](#), *Renew. Energy*, **155**: 604–616 (2020).
- [40] Soltani S., Bonyadi M., Madadi Avargani V., [A Novel Optical-Thermal Modeling of a Parabolic Dish Collector with a Helically Baffled Cylindrical Cavity Receiver](#), *Energy*, **168**: 88–98 (2019).
- [41] Karimi R., Gheinani T.T., Madadi Avargani V., [Coupling of a Parabolic Solar Dish Collector to Finned-Tube Heat Exchangers for Hot Air Production: An Experimental and Theoretical Study](#), *Sol. Energy*, **187**: 199–211 (2019).
- [42] Madadi Avargani V., Rahimi A., Divband M., [Coupled Optical and Thermal Analyses of a New Type of Solar Water Heaters Using Parabolic Trough Reflectors](#), *Sustain. Energy Technol. Assessments*, **40**: 100780 (2020).
- [43] Madadi Avargani V., Rahimi A., Tavakoli T., [Exergetic Optimization and Optimum Operation of a Solar Dish Collector with a Cylindrical Receiver](#), *J. Energy Eng.*, **142**(4): 1–11 (2016).
- [44] Madadi Avargani V., Divband M., [Performance Evaluation of a Solar Water Heating System with Glass-Covered Parabolic trough Concentrators, under Different System Tracking Modes](#), *J. Therm. Anal. Calorim.*, **147**(7): 4873–4888 (2022).
- [45] Madadi Avargani V., B Norton., Rahimi A., Karimi H., [Integrating Paraffin Phase Change Material in the Storage Tank of a Solar Water Heater to Maintain a Consistent Hot Water Output Temperature](#), *Sustain. Energy Technol. Assessments*, **47**: 101350 (2021).
- [46] Madadi AvarganV. i, Norton B., Rahimi A., [An Open-Aperture Partially-Evacuated Receiver for More Uniform Reflected Solar Flux in Circular-trough Reflectors: Comparative Performance in air Heating Applications](#), *Renew. Energy*, **176**: 11–24 (2021) .
- [47] Madadi Avargani V., Rahimi A., Divband M., Zamani M. A., [Optical Analysis and heat Transfer Modeling of a Helically Baffled Cavity Receiver under Solar Flux Non-Uniformity and Windy Conditions](#), *Therm. Sci. Eng. Prog.*, **20**: 100719 (2020).

- [48] Singh R.V., Kumar S., Hasan M.M., Khan M.E., Tiwari G.N., [Performance of a Solar Still Integrated with Evacuated Tube Collector in Natural Mode, Desalination](#), **318**: 25–33 (2013).
- [49] Sivakumar V., Ganapathy Sundaram, E. [Improvement Techniques of Solar Still Efficiency: A Review](#), *Renew. Sustain. Energy Rev.*, **28**: 246–264 (2013).
- [50] Elangovan R., Seeram S R., Radha Krishnan B., Vijayan V., [Experimental Investigation and Parameter Analysis of Solar Still with the Different Wick Materials](#), *Iran. J. Chem. Chem. Eng.*, **41(1)**: 304–309 (2022).
- [51] Bazregari M. J., Norouzi N., Gholinejad M., Fani M., [A 2E Analysis and Optimization of a Hybrid Solar Humidification-Dehumidification Water Desalination System and Solar Water Heater](#), *Iran. J. Chem. Chem. Eng. (IJCCE)*, **41(6)**: 2135–2152 (2022).